Mechanisms of Tryptophan Fluorescence Shifts in Proteins

James T. Vivian and Patrik R. Callis
Department of Chemistry and Biochemistry, Montana State University, Bozeman, Montana 59717 USA

ABSTRACT Tryptophan fluorescence wavelength is widely used as a tool to monitor changes in proteins and to make inferences regarding local structure and dynamics. We have predicted the fluorescence wavelengths of 19 tryptophans in 16 proteins, starting with crystal structures and using a hybrid quantum mechanical-classical molecular dynamics method with the assumption that only electrostatic interactions of the tryptophan ring electron density with the surrounding protein and solvent affect the transition energy. With only one adjustable parameter, the scaling of the quantum mechanical atomic charges as seen by the protein/solvent environment, the mean absolute deviation between predicted and observed fluorescence maximum wavelength is 6 nm. The modeling of electrostatic interactions, including hydration, in proteins is vital to understanding function and structure, and this study helps to assess the effectiveness of current electrostatic models.

INTRODUCTION

Electrostatic interactions (including hydration) are vital to the structure and function of proteins (Hayes and Kollman, 1976; Honig and Nicholls, 1995; Sham et al., 1998; Warshel and Aqvist, 1991; Warshel, 1991). A particularly straightforward method for probing internal electrostatics is the use of a chromophore whose wavelength is sensitive to electric fields. Fluorescence from the amino acid tryptophan has long been known to be sensitive to the polarity of its local environment (Beechem and Brand, 1985; Demchenko, 1986; Eftink, 1991; Konev, 1967; Lakowicz, 1999; Longworth, 1971; Weber, 1960), and is an inviting candidate for such a probe, except that the required microscopic information has not been conveniently accessible.

About 300 papers per year abstracted in Biological Abstracts report work that exploits or studies tryptophan (Trp) fluorescence in proteins. Among the properties used are changes in the fluorescence intensity, wavelength maximum (λ_{max}), band shape, anisotropy, fluorescence lifetimes, and energy transfer. They are applied to folding/unfolding, substrate binding, external quencher accessibility, etc. The power of this probe has been considerably amplified by the finding that Trp can often be substituted for other amino acids by site-directed mutagenesis, with minimal effect on structure and activity. Trp λ_{max} is quite sensitive to its local environment, ranging from ~308 nm (azurin) to ~355 nm (e.g., glucagon) and roughly correlates with the degree of solvent exposure of the chromophore. However, wavelength information, when interpreted, is universally done in a fashion that does not exploit the substantial amount of detail concerning the two lowest excited electronic states of Trp, ^1L_a and ^1L_b, that has emerged from two-photon excitation (Callis and Rehms, 1993; Muiño and Callis, 1994a; Rehms and Callis, 1987; Sammeth et al., 1990, 1992), jet-cooled and argon matrix spectra (Fender et al., 1995; Fender and Callis, 1996; Sammeth et al., 1992), Stark spectroscopy (Pierce and Boxer, 1995), and hybrid quantum mechanical-molecular dynamics simulations (Muiño and Callis, 1994b, c; Callis and Burgess, 1997). What is important here is that the detailed experimental data are well-supported by a variety of semiempirical and ab initio quantum chemical studies (Callis et al., 1995; Chabalowski et al., 1993; Hahn and Callis, 1997; Serrano-Andres and Roos, 1996; Slater and Callis, 1995) [some of this work has been reviewed recently (Callis, 1997)]. Details that should have a substantial impact on Trp spectroscopy are direction of electron transfer and atom charge differences, ^1L_a-^1L_b energy gaps in different environments, detailed vibronic spectra (the ^1L_a transition can have structure), and the effect of broadening upon spectral shape.

These studies (vide supra) have supported the generally held belief that ^1L_a is the fluorescing state in all proteins (with the possible exception of Trp-48 of azurin), and the quantum mechanical studies have—without exception—predicted that electron density is shifted from the pyrrole ring to the benzene ring upon excitation to the ^1L_a state. This means that positively charged residues near the benzene end or negative charges near the pyrrole end of the Trp ring will shift λ_{max} to longer wavelengths (produce a red shift), with the opposite configuration producing a blue shift. Because these shifts are due to the electric field imposed by the protein and solvent, they may be termed an *internal* Stark effect, by analogy to the familiar shifting of energy levels via an applied (external) field.

The internal Stark effect (ISE) has emerged as a useful concept to understand spectral shifts for a wide range of chromophores embedded in a "host" medium, including polyenes (Honig et al., 1979; Kohler and Woehl, 1995), porphryrins (Varadarajan et al., 1989), and other probes (Lockhart and Kim, 1992, 1993; Sitkoff et al., 1994), but has seen little attention for the explanation of Trp fluorescence. This has at least in part been because of uncertainties surrounding the nature of the fluorescing state, which we

Received for publication 13 November 2000 and in final form 31 January 2001.

Address reprint requests to Dr. Patrik Callis, Dept. of Chemistry and Biochemistry, Montana State University, Bozeman, MT 59717. Tel.: 406-994-5414; Fax: 406-994-5407; E-mail: pcallis@montana.edu.

0006-3495/01/05/2093/17 $2.00

feel is no longer an issue. Although not generally recognized as such, the large red shift observed in fluid solvents of high dielectric constant is also a Stark effect, with the strong electric field (reaction field) at the solute being a manifestation of the partial orientation of solvent dipoles around the large solute dipole. A primary contention in the extension of the ISE hypothesis to proteins is that the source of the field is irrelevant; only the magnitude and sign of its projection on the long axis of the indole ring (chromophore) matters in determining the spectral shift.

A pilot study from our group has reported (Callis and Burgess, 1997) preliminary results of hybrid quantum/classical simulations of Trp fluorescence—based purely on this electrostatic effect—wherein a reasonable prediction of λ_{max} was attained for Trps in 16 proteins, starting from the protein crystal, but using only short (2-ps) trajectories and partial solvation. These results served as encouraging evidence for the validity of the internal ISE as a deterministic factor for Trp fluorescence in proteins and the utility of the hybrid simulation approach.

In this paper we refine and extend the previous work (Callis and Burgess, 1997) with full solvation of the protein, longer trajectories, and some scaling of the quantum mechanical charges. This has led to a more satisfactory absolute agreement with experiment and provides a more rigorous test of the ISE hypothesis. In addition, a detailed analysis of the local environment of Trp is provided for several of the proteins.

METHODS

Overview of the simulation procedure and tryptophan environment effects

Our method is an outgrowth of three previous studies: one treating the effect of electric fields in crystals (Sreerama et al., 1994; Theiste et al., 1991), one treating 3-methylindole (3MI) in water (Muiño and Callis, 1994b, c), and one investigating the effect of electric fields in proteins with limited solvation and dynamics (Callis and Burgess, 1997). In the latter and the present work, the most obvious technical challenge is having a way to apply quantum chemistry to a Trp residue that is covalently connected to a large protein. This problem has been dealt with by several groups, often by introducing a "link" atom (see, for example, Lyne et al., 1999). Because in this study we are concerned primarily with the effect of electric fields at the Trp site upon the electronic spectrum, and less about the motions of the Trp, we have chosen to stay with Zerner's spectroscopically calibrated INDO/S method (Ridley and Zerner, 1973) incorporating a modification that allows for input of electrostatic potentials and fields, developed previously and applied successfully in two of our earlier studies.

Our approach to computing Trp fluorescence is a hybrid quantum mechanical/molecular dynamics (QM/MD) technique in which the quantum mechanics is involved only in assigning charges to the Trp ring and C_β and for interrogating the electronic transition energy as a function of the electric potentials produced by the MD force field. The Trp dynamics and atomic coordinates are governed entirely by the MD with QM modified charges on the Trp. The transition energy calculation, with the potentials and fields added, is always performed on a 3MI molecule in a reference ground or excited-state geometry. This procedure uses 196 singly excited configurations, Mataga-Nishimoto electron repulsion screening, and the original CNDO/S overlap factors. The molecular dynamics component of the method is handled by CHARMM (v.26) using the CHARMM22 force field (MacKerell, Jr. et al., 1998).

The effect of the environment surrounding the Trp ring atoms is incorporated directly into the electronic structure calculation through a straightforward modification of the matrix elements of the Fock operator

$$F_{\mu\mu} = F^{(0)}_{\mu\mu} - eV_a \tag{1}$$

$$F_{\mu\nu} = F^{(0)}_{\mu\nu} + e\vec{E}_a \cdot \vec{r}_{\mu\nu} \tag{2}$$

in which e is the electron charge; V_a is the electrostatic potential at quantum mechanical atom a created by all protein and solvent atoms, including Trp backbone atoms; and E_a is the associated electrostatic field. The potential and field are evaluated via straightforward Coulomb sums, using a dielectric constant of unity:

$$V_a = \sum_k q_k / r_{ak} \tag{3}$$

$$\vec{E}_a = \sum_k (q_k / r^3_{ak}) \hat{r}_{ak} \tag{4}$$

where the summations extend over all atoms with the exception of those of the Trp ring and the β-methylene. In practice, the computed electrostatic potentials and fields are applied to a reference 3-methylindole ground- or excited-state structure and orientation, after transforming the field according to the transformation required to rotate the principal moments of inertia of the quantum mechanical Trp atoms from the protein coordinates to the reference orientation.

Electronic excitation of the Trp is simulated by switching the geometry and charges on the reference 3MI to their excited-state (^1L_a) values. Two crucial ingredients for predicting correct fluorescence wavelengths are a realistic geometry change upon excitation and a realistic representation of the intermolecular interactions between the chromophore and environment. For the reference geometries, we currently use a ground state geometry taken from a crystal structure of Trp (Takigawa et al., 1966), while the crucial change in geometry upon excitation is from an ab initio calculation for the 3MI ^1L_a state (Callis et al., 1995), which gave accurate detailed fluorescence band shapes at the vibronic level (Fender et al., 1999). The effect of explicit fields in this procedure is primarily to mix s- and p-orbitals on the same center, with little effect on the transition energies. Most of the internal Stark effect is expressed implicitly by the *difference* of the potentials at different atoms.

Because the 3MI part of the Trp is treated quantum-mechanically, chromophore-protein interactions must be divided into two categories: the potentials and fields due to the surrounding protein that become part of the 3MI hamiltonian, and the potentials and fields produced by the chromophore that act on the protein. For the former, the quantum system sees the protein and solvent simply as a collection of point charges, whose values are taken from the CHARMM22 force field. For the latter, the Trp ring atoms are assigned charges given by the density matrix in the Löwdin basis from the INDO/S calculation:

$$q_A = -e\left(\sum_B P_{BB} - Z_A\right) \tag{5}$$

(where P_{BB} are diagonal elements of the density matrix for all valence atomic orbitals (B) centered on atom A, Z_A is the atomic core charge, and e is the electron charge). Slight adjustments of the Trp β-methylene charges are made to give a net zero charge for the Trp ring group. We have found that the charge distribution of the ^1L_a excited state is sufficiently sensitive to the local field that these charges should be updated every 10 fs to be consistent. The interface for informing the molecular dynamics of the

Trp charges is accomplished by the USERSB subroutine that is native to CHARMM.

We found that using unmodified Löwdin point charges consistently led to overestimation of λ_{max} when the 3MI was solvent exposed, the source of which appears to be short (~1.8 Å) "H-bonds" between the TIP3 model waters and highly negative C4(CE3) and C7(CZ2) atoms of the benzene ring of Trp in the ^1L_a state. Examination of the CHARMM force field reveals relatively "soft" carbon-oxygen Lennard-Jones repulsion parameters, which allows close approach of the water proton to these carbon atoms. The net result of the slightly exaggerated hydrogen bonding in the protein-water (TIP3) simulations is a propensity for overestimated solvent stabilization of the excited-state dipole, which leads to a concomitant overestimated fluorescence red shift. (The CHARMM canonical values for the Lennard-Jones 12–6 parameters for aromatic carbon (CA) and TIP3 oxygen (OT) are $\epsilon = -0.07$ kcal/mol, $R_{min} = 1.9924$ Å and $\epsilon = -0.152$ kcal/mol, $R_{min} = 1.768$ Å, respectively, which are then mixed according to the usual Lorentz-Berthelot combining rules to give a CA–OT minimum at ~3.760 Å, in the absence of Coulomb terms.) Given the gross uncertainties associated with representing the Trp ring charge distribution as Löwdin atomic point charges, we have chosen to empirically scale the charges to give agreement for 3MI in water. A value of 0.80 was found to provide this agreement, and was applied universally before passing the Trp charges to CHARMM.

We emphasize that the charge scaling affects only the MD intermolecular electrostatic interactions between the indole ring and the remainder of the protein and solvent. The primary effect is to reduce the strength of binding of water and/or mobile protein groups to the indole ring during dynamics propagation. The extent of calculated red shifts is indirectly reduced by this scaling only because the average distance between the indole and nearby polar groups is increased, thereby reducing their Coulombic interaction during the QM computation.

An attractive feature to the charge-scaling approach is that it provides a tractable and not entirely unphysical route to good agreement with experiment while avoiding invasive modification of the MD force field and/or electronic structure ingredients. The INDO/S-CIS procedure neglects dispersion contributions and presumably tends to overestimate the partial charges on the Trp moiety. The scale factor corrects for this, albeit in a coarse-grained way.

Finally, the near degeneracy of the ^1L_b and ^1L_a states along with their different polarity creates a practical problem. The energy ordering of the two states frequently interchanges, and the states are often mixed, when the environment is not very polar, making identification of ^1L_a difficult. Determination of which is predominantly the ^1L_a state during the course of the dynamics is made by projecting the ground $\rightarrow$ ^1L_a first-order transition density matrix (Callis, 1984, 1991) for 3MI in vacuum onto the five lowest excited states.

Protein structures, initial conditions, and dynamics

Seed structures for all the proteins (see Table 1) used in this work were obtained from the RCSB Protein Data Bank (PDB) (Berman et al., 2000). The PDB protein structures were pre-processed as follows. The protonation/tautomer state of all histidine residues (HIS) was specified by replacing the HIS residue index with the CHARMM neutral ϵ-H tautomer HSE. A modified PDB file was manufactured to include all crystallographic waters, heteroatoms (e.g., metal ions), and disulfide bonds, as needed, to create a starting structure.

From the starting structures (PDB file), we first added the full complement of hydrogens using the HBUILD command within CHARMM. We then generated fully solvated structures by superimposing on the protein a cube of length 62 Å containing 8000 TIP3 model waters, removing overlapping waters according to a 2.6 Å exclusion radius, and then truncating the cube to a sphere of radius such that all parts of the protein were solvated to a depth of at least 5 Å. A quartic confining potential localized on the surface of the spherical droplet prevented "evaporation" of any of the waters during the course of the trajectory. The fully solvated protein structures were then energy-minimized with 1000 adapted basis Newton Raphson iterations, using a nonbonded interaction cutoff of 10 Å, no electrostatic cutoff, and a dielectric constant of unity.

The resulting fully solvated and energy-minimized structures are taken as the initial configurations for molecular dynamics simulation. A trajectory for a solvated protein is launched with the Trp charge distribution and geometry corresponding to the ground state. Every 10 fs the MD trajectory is interrupted, an electronic structure calculation is performed, and the geometry and charges of the Trp residue are updated. Trajectories were propagated according to the Verlet algorithm (Verlet, 1967) with a time step of 1 fs. The SHAKE (Ryckaert et al., 1977) constraint was applied to bonds containing H. All simulations reported in this work were carried out at a temperature of 300 K. Following 5 ps of ground state dynamics (primarily to ensure equilibration), electronic excitation was initiated by switching the charges and geometry to those of the ^1L_a state, and continuing the trajectory out to (typically) 30 ps, interrupting every 10 fs to perform an INDO/S-CIS calculation and subsequently update the Trp charges.

Harvesting a suitable wavelength to compare with experiment was performed as a straightforward average over the trajectory (transition energy history). To minimize bias due to short-time relaxation effects, the first 1 ps of excited state dynamics was omitted from the average. A detailed examination of transition energy time correlation functions and direct-response results do not reveal a significant relaxation component beyond a few hundred femtoseconds of the ground $\rightarrow$ ^1L_a excitation.

Analysis tools

We have endeavored to decompose the shifts due to protein and solvent environment into contributions from individual amino acid residues, solvent molecules, and in some cases, individual atoms. This can be done effectively at a given point in a trajectory from the scalar projection of the electric potentials at the 3MI atoms and the electron density changes at those atoms accompanying excitation:

$$\sum_{\alpha} V_{\alpha}\Delta\rho_{\alpha} \tag{6}$$

where V_α is computed as in Eq. 3 and the changes in density are taken from the INDO/S-CIS calculation at that configuration. The transition energy shift estimated this way correlates very well with the transition energy shifts coming directly from the program, as they must, given Eq. 3.

Thus, contributions from individual point charges in the environment are given from the individual terms in V_α and these can be summed over individual residues and solvent molecules.

RESULTS

All primary numerical results are contained in Table 1, and most are displayed in Figs. 1–4.

Transition energy histories

Fig. 1, *A–D* displays a sample set of transition energy histories, reported in nanometers, for four proteins: (*A*) azurin (Trp-48), (*B*) subtilisin Carlsberg, (*C*) phospholipase A2, and (*D*) glucagon. This selection portrays the range of influence of Trp environments on fluorescence maxima, encompassing the extremes from Trp "buried" in the interior of the protein (Fig. 1 *A*, azurin Trp-48) to fully solvent

TABLE 1 Proteins, experimental and calculated wavelengths, and computed solvent and protein contributions

Name	PDB Code	Residues (Waters)	Exp.*	Calc (30 ps)	Calc-Exp	Water	Protein	Total	Tot. + 305 nm
Azurin, W48	1AZB	129 (1471)	308	317	9	2	11	13	318
Parvalbumin	1B8R	108 (1603)	316	318	2	13	2	15	320
Myoglobin	1MYT	146 (2964)	321	322	1	1	22	23	328
Subtilisin C.	1SBC	274 (2476)	322	337	15	29	12	41	345
Ribonuc. T1	9RNT	104 (3597)	322	324	2	13	7	20	325
FKBP12	1D6O	107 (3138)	330[†]	316	−14	11	3	14	319
T4-lysozyme, W126	1LYD	164 (2835)	330[‡]	333	3	−6	47	41	346
T4-lysozyme W138	1LYD	164 (2835)	330[‡]	322	−8	−2	27	25	330
T4-lysozyme W158	1LYD	164 (2835)	330[‡]	330	0	45	−8	37	342
Staph. Nuc.	1STN	136 (1393)	334	341	7	−38	97	59	364
Che-Y	1CHN	126 (1467)	335	334	−1	−8	36	28	333
Cobra toxin	1CTX	71 (1777)	340	347	7	29	16	45	350
Phosphlp. A2	2BPP	123 (3129)	340	346	6	51	2	53	358
Monellin	1MOL	94 (3537)	342	351	9	22	41	63	368
Azurin W118	1AZB	129 (1471)	343	337	−6	7	32	39	344
Cholera toxin	1CHP	103 (3055)	345	338	−7	49	−6	43	348
Thioredoxin	2TRX	108 (1569)	345[§]	345	0	8	52	60	365
Melittin	1MLT	26 (1992)	346	348	2	70	−7	63	368
Glucagon	1GCN	29 (3958)	352	354	2	42	20	63	368
3MI		1 (289)	365[¶]	364	−1				
Vacuum			295[‖]	305	10				

*From Eftink (1991) unless otherwise referenced.
[†]Egan et al. (1993).
[‡]Harris and Hudson (1991).
[§]Callis et al. (2000).
[¶]P. Callis, unpublished data.
[‖]Estimated from Sammeth et al. (1992).

exposed (Fig. 1 *D*, glucagon). Subtilisin Carlsberg (Fig. 1 *B*) and phospholipase A2 (Fig. 1 *C*) represent two types of intermediate cases of a Trp that is partially exposed to water. Subtilisin C is pathological in the sense that its average predicted λ_{max} value shows one of the greatest deviations from experiment, along with large, low-frequency fluctuations in calculated λ_{max}.

During the first 5 ps of these trajectories, the Trp is in the ground state, meaning we use the ground state geometry and the indole charges used by CHARMM are those computed for the ground electronic state (scaled by 0.8). During this part of the trajectory, transition energy means vertical absorption energy, and should correlate with the UV absorption λ_{max}. Following the first 5 ps, Trp is in the ^1L_a excited state, and transition energy means vertical fluorescence energy, which should correlate with the fluorescence λ_{max}. The abrupt discontinuity at ~5 ps results from shifting the geometry of the 3MI from the ground to the excited (^1L_a) values and defines the instantaneous Stokes shift between absorption and fluorescence. When there are several water molecules within ~10 Å of the Trp, relaxation of the waters in response to the increased dipole of the Trp can be seen out to ~500 fs. The high frequency fluctuations (~20 fs time scale) of the transition energy are due predominantly to the now well-understood rapid inertial water motions in the region near the chromophore (Jimenez et al., 1994; Maroncelli, 1993). In addition, some relatively long-time fluctuations (several picoseconds) are manifest in the transition energy histories that reflect the influence of large-amplitude motions of the protein backbone and side chains and/or wholesale rearrangement of nearby H-bonded water clusters.

Fig. 2 illustrates the effect of scaling the quantum mechanical Trp ring charges by 0.80. Fig. 2 *A* shows the extracted λ_{max} (fluorescence band maxima in nanometers) for the collection of proteins, compared to experiment, using *unscaled* INDO/S charges on the chromophore. As benchmarks for comparison, we also include the wavelengths for 3MI in vacuum (from INDO/S) and fully solvated with TIP3 waters using the same hybrid QM/MD simulation approach as for the proteins. The vacuum and fully solvated 3MI results serve as theoretical reference points for the protein data series; the vacuum result is a prototype for a completely isolated chromophore, while the fully solvated 3MI represents a model for a Trp residue whose fluorescence wavelength is determined entirely by the water reaction field.

All of the proteins in Fig. 2 *A* exhibit Trp fluorescence maxima between the vacuum and fully solvated 3MI limits and the wavelengths correlate at a qualitative level with the experimental values. The most obvious aspect of disagreement is the general overestimation of λ_{max} for those Trps exposed to water, epitomized by the fully solvated 3MI result. The mean unsigned absolute error in the calculated

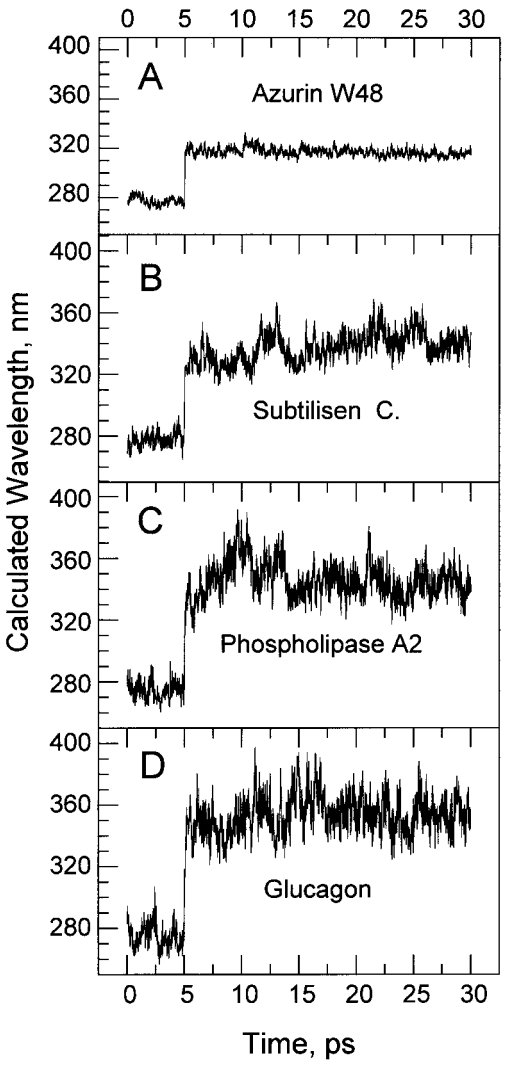

FIGURE 1 Plots of calculated transition wavelength versus time during the dynamics trajectories for a selection of four proteins. During the first 5 ps the indole ring charges and geometry are those for the ground state. During the following 25 ps the indole ring charges and geometry are those for the ^1L_a excited state. Every 10 fs the transition energy is computed and the indole ring charges are updated in the CHARMM database. (*A*) Trp-48 of apo-azurin. (*B*) Trp-113 of subtilisin Carlsberg; (*C*) Trp-3 of phospholipase A2; (*D*) Trp-25 of glucagon.

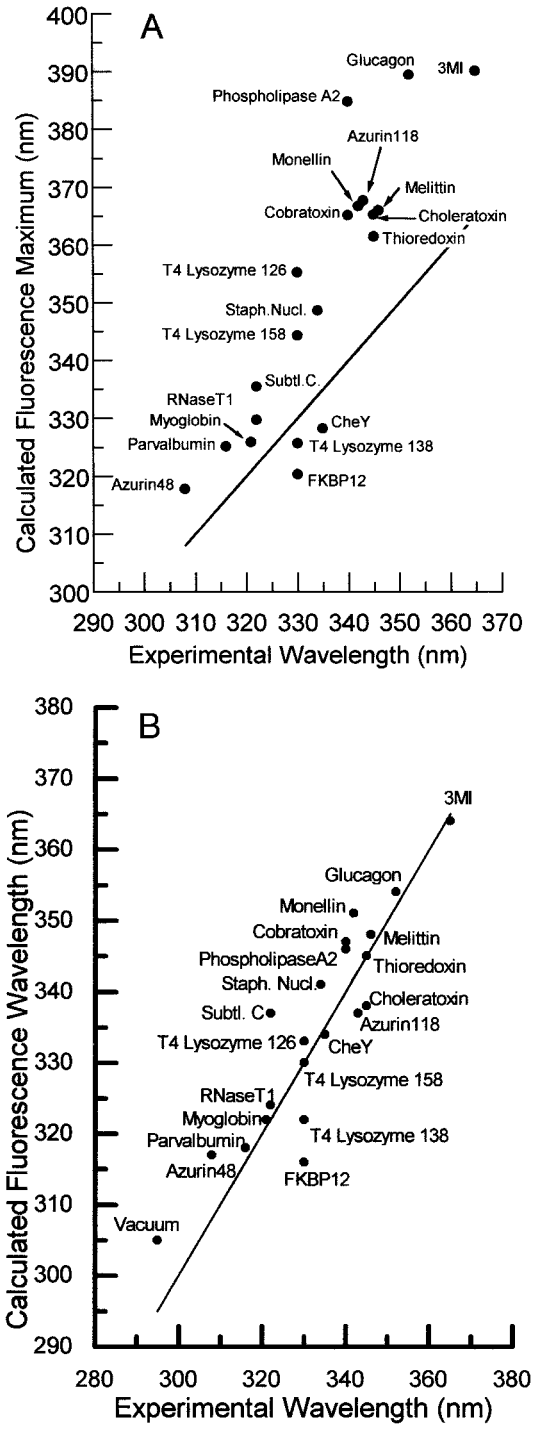

FIGURE 2 Plots of calculated versus experimental fluorescence maximum wavelengths for 19 Trps in 16 proteins and for 3-methylindole in water. (*A*) Charges on the Trp ring are not scaled and the calculated values are averages over the 400 values during 4 ps of excited-state trajectory. (*B*) Charges on the Trp ring are multiplied by 0.80 and the calculated values are averages over the 2400 values calculated during the last 24 ps of trajectories of the type shown in Fig. 1.

values is 17 nm. The general results in Fig. 2 *A* are quite similar to those of the preliminary study (Callis and Burgess, 1997), which used the consistent valence force field (CVFF) (Lifson et al., 1979) with the Discover MD program (Molecular Simulations, Inc., San Diego, CA), except that the overestimation of interaction with water is somewhat higher using CHARMM.

Fig. 2 *B* shows the average wavelengths from a separate set of production runs for which the INDO/S computed Trp ring charges—as seen by CHARMM—are scaled by 0.80. This only affects the CHARMM energy functions, leading to increased equilibrium distances between the Trp ring

atoms and solvent and protein atoms with large atomic charges, thereby reducing the magnitude of any red shifts resulting from relaxation of solvent and mobile protein groups (e.g., lysine side chains) in response to the charge redistribution during excitation. Substantially better agreement with experiment is captured, relative to the unscaled charge results, with the mean unsigned absolute error now being only 6 nm. Noteworthy is that the most red-shifted proteins of the set, glucagon and phospholipase A2, are brought into more reasonable agreement with experiment. Similarly, the bulk of the intermediate wavelength proteins—from parvalbumin to melittin—display substantial improvement. Notably, the three Trps of T4-lysozyme (W126, W138, W158), which exhibit a spread of 30 nm in the unscaled charge results, are within 11 nm upon scaling the charges. Interestingly, che-Y, which is blue-shifted relative to experiment with unscaled charges, is actually brought into reasonably good agreement with scaling, while FKBP12 (FK506 binding protein) remains blue-shifted. Cases wherein Trp is buried and isolated from mobile polar groups should not be affected by the scaling, and indeed little effect is seen.

A few comments are warranted on the sensitivity of the final results with respect to the simulation protocol as outlined in the Methods section. The meticulous inclusion of the crystallographic waters, metals, and disulfide bonds generally proved not to be a decisive factor in determining an accurate fluorescence wavelength. Che-Y is an exception, where inclusion of Mg^{2+} contributes a $\sim$20 nm blue shift. Typically, inclusion of the crystallographic waters changed the calculated result by no more than 4 nm. For T4 lysozyme W138, however, their inclusion led to a substantially different conformation of the nearby Gln-105 and Arg-145, with a consequent 15 nm blue shift. In addition, the general agreement of predicted with experimental wavelengths was insensitive to the length of the ground state trajectory and the excited-state trajectories accessible to us, except for a few cases exhibiting extreme environmental fluctuations, as shown in Fig. 1. Finally, we note that although the results presented here are based on single trajectories, one trajectory for each protein, a survey of trajectory-averaged results for a subset of the proteins studied here displayed little sensitivity to the number of trajectories.

Solvent versus protein shifts

An interesting question is to what extent the fluorescence λ_{max} is governed by solvent and protein residues. Our method does allow this formal division, but we acknowledge at the outset that this distinction is muddied by two types of coupling that occur within our model: 1) orientational polarization of the water by charged and polar protein residues, and 2) electronic polarization of the Trp ring by electric fields from both water and protein. We shall see a number of cases wherein oriented regions of water containing hundreds of water molecules 15–25 Å from the Trp collectively contribute 5–10 nm red and blue shifts. These are apparently due to domains of water ordered by charged groups in the protein, and are therefore indirectly caused by protein. The second type of coupling arises because the shift in transition energy depends upon the change in dipole upon excitation, and because the dipole change is increased by fields that create a red shift (fields that force electrons in the direction of electron transfer). Thus, the contribution by *both* protein and water increases with increasing wavelength.

Fig. 3 shows an estimated decomposition of the spectral shifts relative to vacuum, in nanometers, for each of the members of Fig. 2 *B*, segregated into contributions from the solvent and non-Trp residues of the protein and arranged from shortest to longest average wavelength for the constituent proteins. This was done using Eq. 6 and the analysis tool described in the Methods section (red shifts correspond to positive values, while blue shifts are reported as negative, and the sum of the solvent and protein contributions defines

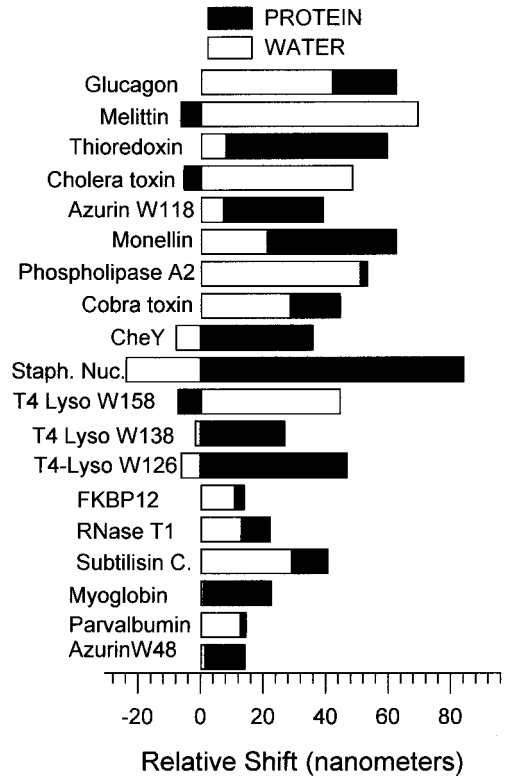

FIGURE 3 Estimated decomposition of the spectral shifts relative to vacuum, in nanometers, for each of the members of Fig. 2 *B*, segregated into contributions from the solvent and non-Trp residues of the protein and arranged from shortest to longest average wavelength for the constituent proteins. This was done using Eq. 6 and the analysis tool described in the Methods section. Red shifts correspond to positive values, while blue shifts are reported as negative, and the sum of the solvent and protein contributions defines the net shift.

the net shift). Curiously, although the shifts do not exhibit monotonic behavior for solvent or protein contributions, there is clearly a propensity for red shifts from both sources. Of the entire series of 19 Trps, only three (T4-lysozyme W126, Staph. nuclease, and che-Y) show a significant blue-shifting contribution from solvent, and only three (melittin, T4-lysozyme W158, and cholera toxin) display contributed blue shifts arising from the protein residues. We comment in some detail on the significance of this result in the Discussion section.

Mechanism of shifts caused by water

These may be divided roughly into strong, close-range interactions involving a few first solvation shell molecules, and longer-range effects of the reaction field type involving hundreds of molecules. The reaction field could be mostly due to the ^1L_a dipole, as for 3MI, glucagon, and melittin, or could be primarily shaped by the collection of charged residues of the protein. When the reaction field is due to the excited-state dipole, it will always lead to a red shift when the excited state dipole is larger than the ground state dipole (Onsager, 1936). However, if it is mainly due to other charges in the protein, the shift can be of any sign and magnitude.

With our hybrid model, a single water can donate an H-bond to the π cloud of the benzene ring of ^1L_a excited 3MI. These have binding energies of ~11 kcal/mol in the ^1L_a state and ~2–3 kcal/mol in the ground state using the scaled charges at 0 K. In the π-complex, the computed fluorescence red shift is 1500 cm^{-1} (15 nm). For the σ-complex, wherein the HN donates a hydrogen bond to water, the computed red shift is ~10 nm. Because the interaction and shifts are much larger for the ^1L_a state than for the ground state, they are reminiscent of the excited-state complexes ("exciplexes") postulated by the Lumry group (Hershberger et al., 1981; Walker et al., 1967). However, as will be discussed below, they have much different structures. Other configurations leading to significant shifts have favorable dipole-dipole interactions, with the dipole of water opposing that of the indole in a side-by-side arrangement or with the dipoles parallel in an end-to-end arrangement. Model calculations incorporating scaled charges show that these specific configurations give red shifts of ~8–10 nm and ~3–5 nm, respectively, relative to the computed transition energy in vacuum (305 nm), and they give corresponding blue shifts when the dipole of the water is reversed. These dipole-dipole interactions become weaker as the cube of the intermolecular distance, but the number of water molecules increases rapidly with increasing distance, so that long-range contributions from weakly ordered (reaction field) water can be quite significant.

When individual water contributions are determined in the protein/solvent environment, contributions as large as 2400 cm^{-1} (~24 nm) are found, i.e., much larger than can be obtained with a single water + 3MI. The reason for this is that the ^1L_a excited state is quite polarizable. When several waters are contributing to a red shift, as is always the case for a solvent-exposed Trp, the ^1L_a transition has much more electron transfer from the pyrrole to the benzene ring. For example, the change in dipole is 4.82 Debye, ~7 D, and ~8 D for red shifts of 0 (^1L_a 3MI in vacuum), 36 nm (FKBP12), and 117 nm (glucagon), respectively. [These anecdotal examples are chosen simply to illustrate the broad range of behavior in shifts versus dipole change, which were noted previously (Muiño and Callis, 1994b).] Thus, a high degree of polarization of the ^1L_a state means that the individual contributions of all interacting residues is amplified, i.e., both red and blue shifts will be magnified for the highly polarized cases.

Fig. 4 shows a sampling of plots of integrated average contributions to the fluorescence shift from all waters within a distance, *r*, from the Trp as a function of *r*. The range of behavior is surprisingly large, and cannot be predicted from apparent exposure to water. For example, the Trps of Staph. nuclease, subtilisin Carlsberg, and Trps-126,158 of T4-lysozyme all appear to lie on the surface with one edge of the Trp exposed to water, but the average water contribution varies from a 40 nm blue shift to a 45 nm red shift. Even for completely buried Trps such as in azurin (W48) and parvalbumin, there may or may not be substantial long-range contributions from water. In addition, it is interesting that the sign and magnitude of the contributions is seen to depend on distance.

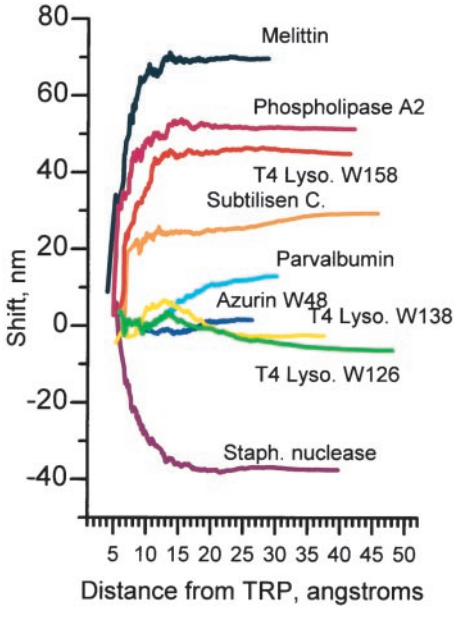

FIGURE 4 Selected plots of integrated average contributions to the fluorescence shift from all waters within a distance, *r*, from the Trp as a function of *r*. The range of behavior is surprisingly large, and cannot be anticipated from apparent exposure to water.

The short-range exciplex interaction with water is most pronounced for melittin, as can be seen in Fig. 4. On average, three waters are residing at <5 Å from the Trp and making a total shift of 27 nm. Other highly exposed Trps are those in phospholipase-A2, cobra and cholera toxins, monellin, Trp-118 of azurin, and glucagon, which typically are on average only making one or two strong, short-range interactions. Trp-158 of T4-lysozyme almost never makes an exciplex, presumably because of its lack of an exposed face.

A variety of reaction field-type contributions are evident in Fig. 4. Melittin, phospholipase A2, and Trp-158 of T4-lysozyme exhibit close to classic reaction field-type behavior, with large red shifts due to orientation of water in reaction to the Trp dipole change. Choleratoxin and glucagon (not shown) behave similarly. More often, there appear to be striking reaction field effects produced by the protein. In Fig. 4, parvalbumin, Staph. nuclease, Trp-126, and Trp-138 of T4-lysozyme show contributions on the order of 10 nm from waters beyond 10 Å. In addition, ribonuclease-T1, Trp-118 of azurin, FKBP12, che-Y, apo-myoglobin, and Trp-28 of thioredoxin show this behavior. The complexity and range of behaviors point to domains of ordered water in response to the individual protein charge distributions and shapes, as has been recently reported by Higo et al. (1999).

An interesting question is, What are the temporal durations of the strong associations between water and the Trp ring in this model? For glucagon, the water making the dominant average red shift (9 nm) is in the first or second solvation shell for the entire excited-state trajectory (25 ps). Its contribution varies from red shifts of 24 nm to blue shifts of 12 nm. When it is making the $+24$ nm shift, it is donating an H-bond to the π cloud, with H in the center of the benzene ring. When making the largest blue shift, this water has moved <1 Å, so that one H is over the pyrrole ring while the O is over the benzene ring. Similar behavior is found for the dominant red-shifting waters in the melittin simulation. The strongly red-shifting waters commonly will make 15 nm red shifts over a period of 5 ps, but during this time there may be 0.1 ps intervals during which the red shift is nearly zero.

Mechanism of shifts caused by protein

Protein contributions may be classified as being from charged side chains, polar side chains, Trp backbone, and other backbone. All charged residues can make significant contributions because of the long-range nature of the Coulomb interaction of a point monopole and a point dipole. The formula for such an interaction is:

$$2q\Delta\vec{\mu}\cdot\vec{r}/r^3 \tag{7}$$

which gives a 600 cm^{-1} ($\sim$6 nm) shift for a unit charge lying on the long axis of Trp 20 Å distant when the change in dipole is 5 Debye. Polar side chains and backbone typically contribute shifts of 5–10 nm primarily by a dipole-dipole mechanism, but only at short range (van der Waals contact). Some extreme cases, however, reach 20 nm.

For virtually every protein examined in this study a charged amino acid residue (Lys, Arg, Asp, Glu, and any N- or C-terminal residue) makes the largest contribution to the computed fluorescence shift. Usually there is considerable cancellation of red and blue shifts. The largest red shifts at a particular configuration observed were 78 nm for Lys-133 of Staph. nuclease and 67 nm for Asp-26 of thioredoxin; the largest blue shift contributions observed were 39 nm for Lys-57 in thioredoxin and 38 nm from Arg-22 in melittin monomer.

The largest shifts found with this model due to neutral side chains were 20 nm from Asn-117 of subtilisin Carlsberg and 7 nm for Gln-105 of T4 lysozyme (W-138). The amide induced shift from Asn-117, which is in direct contact with one face of the Trp ring, ranges from a 12 nm blue shift to a 20 nm red shift, depending on its χ_2 rotamer conformation.

The Trp backbone atoms contribute significantly, but never dominate. On average these contributions range from a 9 nm blue shift (for Trp-118 of azurin) to a 6 nm red shift (for monellin). The shifts arise from a variety of ϕ-ψ-χ_1-χ_2 combinations, with blue shifts being about three times more common.

Non-Trp backbone contributions are normally only a few nanometers, but an average red shift of 17 nm is found for Pro-60 in ribonuclease T1, because a unique combination of dihedral angles places both the N and O near the pyrrole ring of Trp-59.

Classification

Tryptophans in the proteins studied here fall roughly into five classes (see Table 2) at the present level of analysis.

TABLE 2 Classification of tryptophan environments

Class	Description	Cases
1	Buried, no exposure to water	azurin W48, ribonuclease T1, myoglobin, che-y, T4 lysozyme W138, parvalbumin
2	Edge exposed	subtilisin C., T4 lysozyme (W126 and W158), Staph nuclease
3	One face only	FKBP12
4	One face and edge exposed	phospholipase A2, cobra toxin, cholera toxin, monellin, azurin W118
5	Two faces and edge exposed	glucagon, melittin

What is important appears to be the extent of exposure of the *faces* of the benzene part of the Trp ring, because stabilization by water is most effective through the close approach of water protons to C4(CE3) and C7(CZ2). Waters at an edge or at the face of the pyrrole ring are unable to interact strongly enough to create a large red shift, and the orientation of these waters is often more strongly influenced by neighboring polar groups than by the ^1L_a dipole. The relationship between our results and the proposal of discrete environmental states by Burstein et al. (1973) will be explored in the Discussion section.

Selected cases

Azurin (Trp-48) (see Fig. 1 *A*) is exceptional in several respects. Within the current catalog of measured protein fluorescence spectra (Eftink, 1991) it is the least red-shifted member, owing to Trp-48 being well-buried in the interior of the protein within an entirely hydrophobic pocket. Although the fluorescence spectrum is very similar to that of 3MI in pure hydrocarbon solvents (Burstein et al., 1977; Szabo et al., 1983), our results show that this is largely due to cancellation of moderate electrostatic interactions, leaving a residual red shift of ~12 nm. The magnitudes of the transition energy fluctuations in this case are small (relative to all other proteins examined), reflecting the fact that both water and charged groups are denied close access to the chromophore. Water is rarely found <9 Å from Trp-48, as can be seen in Fig. 4.

Glucagon (Fig. 1 *D*) represents the extreme of a fully solvent-exposed Trp, and a histogram of TIP3–Trp-27 distances demonstrates that the closest approach is ~3.5 Å, quite similar to the ~3.76 Å predicted for Lennard-Jones interaction between typical aliphatic carbons and the TIP3 oxygen. Both faces are well exposed. Thr-29 (C-terminus) and Asp-21 are the corresponding residues above and below on the helix, and both have carboxylates near the pyrrole ring, the primary reason for the 20 nm red shift from protein. Water contributions are mainly due to the classic reaction field from the ^1L_a dipole, but a 6 nm blue shift from waters beyond 15 Å indicates that the reaction field is partly shaped by the protein.

FKPB12 represents a case where we fail to come within 10 nm of experiment. Trp-59 lies at the bottom of a hydrophobic cavity (the binding site of the immunosuppressant FK506) with one face completely exposed to water. However, only about 1 or 2 waters are able to H-bond to the face at any given time. Sometimes the waters form a hydrogen-bonded "ring" structure, wherein the water-water interactions are more favorable than water-Trp interaction for significant periods over the course of the full trajectory, thereby accounting for the small average red shift. About 100 waters 7–15 Å from the Trp give a net 8 nm red shift and ~3000 waters 15–30 Å away give a net 8 nm blue shift.

Fig. 5 shows Trp-19 and its near neighbors in melittin monomer after 30 ps of dynamics, along with the six waters making the strongest interactions in this frame. Lys-23 and Trp-19 come off the same side of the helix, with the Lys NH_3^+ over part of the benzene ring. Water can reach most of this face and all of the other side, resulting in a classic reaction field profile, with an average 60 nm red shift from waters 4.5–9.0 Å from the Trp. Lys-23 gives a large red shift, but Arg-22 gives a larger blue shift, on average. Because the structure is a single helix, other residues are not effective. The red-white waters are making red shifts of 13–18 nm, except for the one accepting the H-bond from the Trp HN, which has its dipole perpendicular to the Trp ring; it contributes a 2 nm red shift. The cyan water makes a blue shift of 6 nm. These are the major players of the closest nine waters in this frame; in total they contribute an 81 nm red shift, with Lys-23 on the left and Arg-22 on the right contributing 30 nm red and blue shifts, respectively. The protein contributes a net zero in this frame.

Fig. 6 *A* shows Trp-140 of Staph. nuclease, 25.70 ps into the dynamics (waters removed from view) illustrating apparent water exposure and the close contact of three lysines. Lys-110 and Lys-133 are close to the benzene ring and contribute a combined shift of 95 nm in this frame, while Lys-136 contributes a 7 nm blue shift. Fig. 6 *B* shows the same perspective somewhat closer, but with only those waters within 11 Å of the Trp and the amino groups of the nearby lysines. The cyan colored waters all contribute a blue shift and the red-white waters contribute red shifts. The blue-shifting waters are primarily in chains terminating on the red-shifting lysines. Many of the red-shifting waters are in chains that terminate on the blue-shifting Lys-136.

Trp-113 of subtilisin Carlsberg is interesting because it is apparently solvent-exposed, yet has a very blue-shifted

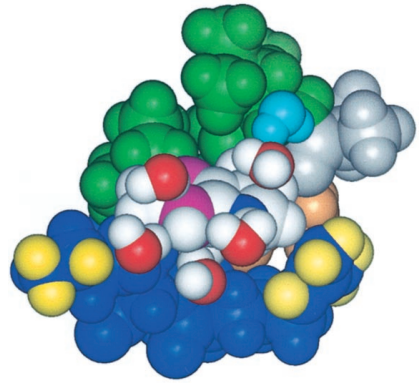

FIGURE 5 Trp-19 of melittin after 25 ps of excited-state dynamics. The red-white waters are making red shifts of 13–18 nm, except for the one accepting the H-bond from HN, which has its dipole perpendicular to the Trp ring and contributes a 2 nm red shift. The cyan molecule makes a blue shift of 6 nm. These are the major interactors of the closest nine waters, which contribute an 81 nm total red shift. Lys-23 on the left and Arg-22 on the right contribute 30 nm red and blue shifts, respectively. The protein contributes a net zero in this frame.

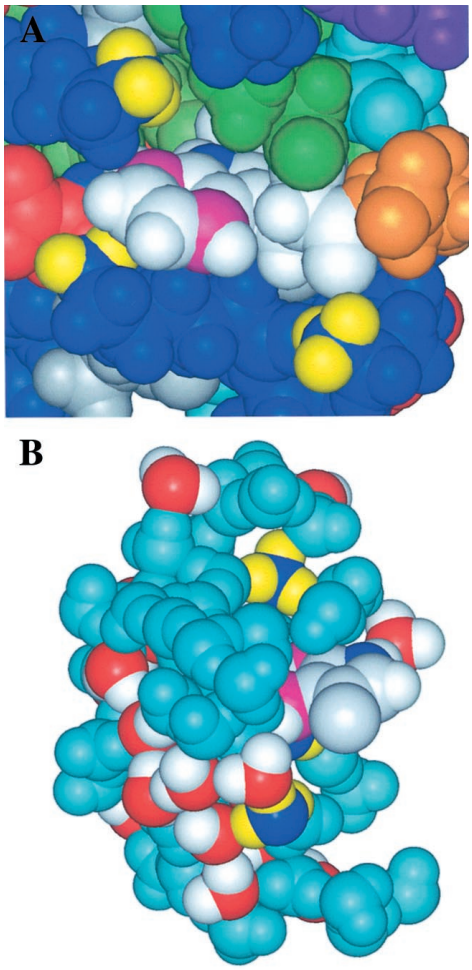

FIGURE 6 (*A*) Trp-140 of Staph. nuclease is shown in cpk color, except that C4(CE3) and C7(CZ2) are shown in purple. The HZ hydrogens of the nearby lysines 133, 110, and 136 are shown in yellow. Note that Lys-133 and Lys-110 lie over and under the benzene ring of the Trp, contributing a combined 96 nm red shift. (*B*) The same view as (*A*) showing only water within 11 Å. The cyan waters contribute a blue shift in this frame and the red-white colored waters contribute red shifts. The ammonium groups of Lys-133, Lys-110, and Lys-136 are also shown.

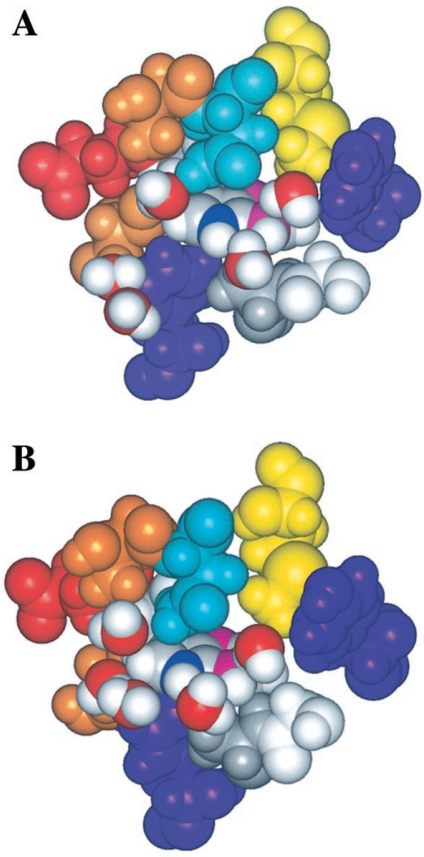

FIGURE 7 Frames at 10.8 (*A*) and 13.0 ps (*B*) into the dynamics trajectory for subtilisin Carlsberg. These frames were picked to show the cause of the large increase (317 to 364 nm) in the calculated wavelength during this interval (see Fig. 1). The waters shown are just those that make at least a 5 nm contribution to the increase. The water making the H-bond to CZ2 of the Trp-113 in (*B*) is making a 17 nm red shift, but only 0.3 nm in (*A*). In addition, the backbone of Gly-47 and Ala-48 also contribute to the increase. Asn-117 (*cyan*) lies in van der Waals contact above the Trp ring, and was seen to make a χ_2 flip during the trajectory. In doing so its contribution to the shift changed from a 12 nm blue shift to a 20 nm red shift.

λ_{max}, which our calculations fail to capture. In addition, its trajectory (Fig. 1) shows large excursions. Fig. 7, *A* and *B* show frames at 10.8 and 13.0 ps into the dynamics trajectory for subtilisin Carlsberg. These frames were picked to show the cause of the large increase (317 to 364 nm) in the calculated wavelength during this interval (Fig. 1). The five waters shown are just those that make at least a 5 nm contribution to the *increase*. The water making the H-bond to CZ2 of Trp-113 in Fig. 7 *B* is making a 17 nm red shift, but only 0.3 nm in Fig. 7 *A*. In addition, the backbones of Gly-47 and Ala-48 contribute to the increase. An interesting sidelight is that Asn-117 lies in van der Waals contact above the Trp ring, and was seen to make a χ_2 flip during the trajectory. In doing so, its contribution to the shift changed from a 12 nm blue shift to a 20 nm red shift. However, this had little effect on the overall shift. The close proximity of this residue is a possible reason for the low quantum yield and short fluorescence lifetime for this Trp. The Asn side chain has been shown to have a significant quenching effect on 3MI in solution (Chen and Barkley, 1998).

Finally, we note some details of the results for ribonuclease T1 for the purpose of comparison with the elegant 50 ps ground state simulation reported by Axelsen and Prendergast (1989), a simulation specifically aimed at gaining microscopic understanding of the fluorescence spectra and lifetime. The crystal waters WAT-107, 108, and 191 of the 9RNT structure used here correspond to 112, 142, and 114, respectively, of 1RNT used in their study. We find, as did they, that these waters remain very near their crystal positions during a 50 ps trajectory. WAT-107 spends the entire trajectory donating H-bonds to O of Pro-60 and WAT-108

and accepting one from Tyr-68. Much of the time WAT-107 is unable to accept an H-bond from the Trp HN because its O lies above C7 of the Trp benzene ring. In this configuration, WAT-107 contributes a blue shift of up to 12 nm. Some of the time WAT-107 does accept the Trp HN H-bond, during which time it contributes up to a 4 nm red shift. The average contribution in the excited state by WAT-107 is a 2.5 nm blue shift, and its behavior in the ground state is not significantly different. We have consistently found that the dominant red shift contribution comes from Pro-60, whose O and N lie close to the pyrrole ring of the Trp. The red shift ranges from 8 to 25 nm in the excited state and the average is 17 nm. The ground-state behavior is not significantly different. We agree with the early study (Axelsen and Prendergast, 1989) that the environment of Trp-59 is surprisingly polar considering its observed blue-shifted fluorescence (322 nm); our findings provide a reasonable proposal for the underlying reason.

Calculated absorption shifts

Shifts in absorption spectra are typically much smaller than the corresponding fluorescence shifts, both experimentally and in our calculated results. The reason is largely because the solvent reaction field at the time of excitation is dictated by the much smaller *ground state dipole*. In addition, the change in dipole upon excitation is smaller because the ^1L_a state is not as polarized. The calculated absorption shifts relative to vacuum ranged from -1 to $+14$ nm, whereas the calculated fluorescence shifts ranged from $+11$ to $+49$ nm. There was poor correlation between the absorption and fluorescence shifts, as might be expected because of the differing contributions from water that can respond to the excited state dipole and that which cannot. In this paper we do not attempt comparison of experimental and calculated absorption shifts because of the difficulty in accurately locating the ^1L_a absorption maximum, which is overlapped by Trp ^1L_b (and often by tyrosine) absorption.

DISCUSSION

New concepts arising from this study

Directional interaction

This work provides a rational framework upon which to interpret fluorescence wavelength changes for tryptophan in proteins. The agreement of prediction and experiment is sufficient to affirm the basic concept that the local electric field direction and magnitude primarily determine the sign and magnitude of the shifts relative to vacuum. Being near a charged group or dipolar group does not mean there will be a red shift; the relative orientation of the charge or dipole to the ring determines whether there will be a red shift, a blue shift, or no shift at all. In particular, the unanimous results of numerous quantum mechanical treatments are authenticated by the collective agreement demonstrated here. In particular, for these proteins the fluorescent state is ^1L_a (with the possible exception of Trp-48 of azurin) and the electron transfer is from the pyrrole to the benzene ring for the ground ($^1A_1$) $\rightarrow$ ^1L_a transition. This behavior was actually pointed out in a few earlier studies, but has been generally ignored (Andrews and Forster, 1972; Ilich and Prendergast, 1991).

Blue shifts from water

Currently, the most common use of Trp fluorescence λ_{max} information is to assign a Trp as buried and in a "non-polar" environment if λ_{max} is $<\sim$330 nm; if λ_{max} is longer than $\sim$330 nm, the Trp is assigned a "polar" environment, which almost always is intended to imply solvent exposure. The model presented here shows that mere exposure to water may or may not create a large red shift. Again, the *relative* orientation of the water dipole to the ring determines whether there will be a red shift, a blue shift, or no shift at all.

Long-range shifts from protein-ordered water

As seen in Fig. 4, significant shifts due to the collective effect of many ordered waters are found in this study. Presumably, the influence of charged residues distributed throughout the protein structure play an important role in determining the wholesale ordering of the water, and a recent study by Higo et al. (1999) offers a beautiful illustration of the effect and consequences on water self-diffusion. We are currently investigating the systematics of this interesting effect.

Necessity for explicit solvent: exciplexes

The nature of the often-invoked exciplexes is made quite specific in this work. The idea of exciplexes grew from observations by Mataga et al. (1964) and by Lumry and co-workers (Walker et al., 1967; Hershberger et al., 1981) that millimolar concentrations of alcohols, when added to a solution of indole or 3-methylindole in pure hydrocarbon, would cause considerable shifts in fluorescence while causing minute changes in the absorption. Although Mataga suggested that the interaction was similar to an Onsager-type reaction field, Hershberger et al. (1981) advanced a rather detailed picture of two binding sites: an electrophilic one at C3(CG) and a nucleophilic one at N1. To date, however, all quantum mechanical treatments suggest that the considerable electron transfer to the benzene ring upon excitation to ^1L_a would lead to an electrophilic site (or sites) on the benzene ring.

Traditionally, the term exciplex has implied a repulsive ground state, and therefore no significant complexation in the ground state. There is some evidence that this is not the

case, even for indoles in hydrocarbon-alcohol solvents (Skalski et al., 1980) (V. Wagner and P. R. Callis, unpublished results). The exciplex behavior seen in our model for the protein-Trp interactions is qualitatively different, however, and should more accurately be termed relaxation. That is, there is significant interaction already in the ground state; this interaction becomes stronger in the excited state because of shortened distance between the interacting groups due to relaxation The complexes leading to the largest single water-induced shifts are the most exciplex-like, because they are much less common in the ground state. It is rare to find a single water-induced red shift >5 nm for an exposed Trp when the solvation shell is in response to the ground state, but common to find shifts of 20 nm shortly after excitation. However, unlike the specifically localized exciplexes of Hershberger et al. (1981), we find a wider locus of positions/orientations that can cause large red shifts. Our use of explicit solvent instead of a dielectric continuum has provided rich detail regarding close-range exciplex-type interaction that would be highly distorted in a continuum approach, wherein the results would be dependent upon an arbitrary cavity about the Trp and choices of the controversial protein dielectric constant, as well as some of the inherent problems associated with grid-based electrostatic approaches (e.g., Poisson-Boltzmann treatments). Presumably, the longer-range effects due to the reaction field of bulk water to protein charges would be represented reasonably well in continuum models (Tannor et al., 1994), for example, or the microscopic protein dipoles Langevin dipoles (PDLP) of Warshel and co-workers (Florian and Warshel, 1997), but the short-ranged and highly specific interactions between water and proximal residues with the chromophore are crucial ingredients for the level of microscopic detail required to rationalize the spectral shifts.

Comment on the discrete state model of Burstein

Some time ago, Burstein and co-workers (Burstein et al., 1973; Reshetnyak and Burstein, 1997) proposed that all Trp fluorescence spectra in proteins could be described as a superposition of five discrete basic spectra emanating from five distinct local environments: A, no exciplexes (λ_{max} = 308 nm); S, 1:1 exciplex (λ_{max} = 316 nm); I, 2:1 exciplex in interior (λ_{max} = 331 nm); II, on surface in contact with bound water (λ_{max} = 340–342 nm); and III, on surface in contact with mobile water (λ_{max} = 350–353 nm). This proposal was based on observations of the spectral widths of the fluorescence of Trp in proteins, which very often did not fit the correlation of bandwidth with λ_{max} found for indole in a wide variety of solvents. Although we certainly can agree with the class A and class III categories, our results at this stage do not seem to fit the other classes so well. For example, the four S-class cases (parvalbumin, ribonuclease T1, subtilisin C., and apo-myoglobin) gain their red shift relative to A-class by quite different mechanisms. Ribonuclease-T1 has an average red shift from water of 10 nm in the ground state, increasing to 14 nm in the excited state. The nearby crystallographic waters are simply too involved in H-bonding to backbone atoms to form exciplex-like interactions with the Trp. The backbone of Pro-60 contributes an average 14 nm red shift in the ground state and a 17 nm red shift in the excited state; a small relaxation rather than exciplex formation. Parvalbumin differs from azurin (W48) only by a 12 nm red shift contributed from hundreds of waters >10 Å from the Trp, a reaction field dictated by the protein having no apparent exciplex component. Apomyoglobin has almost no shift from water and a 22 nm red shift from protein in both the ground and excited states.

How realistic is the model?

INDO/S-CIS has proven effective in a large number of cases, including our previous studies (Muiño et al., 1992; Muiño and Callis, 1994b, c; Sreerama et al., 1994) and in several impressive applications to large systems, some similar to ours. Some examples include hybrid simulations of the photosynthetic reaction center (Gehlen et al., 1994; Marchi et al., 1993; Thompson and Zerner, 1991; Thompson and Schenter, 1995), path integral molecular dynamics simulations of tryptophan in water (using CNDO/S) (Simonson et al., 1997), electronic spectra of uracils (Broo et al., 1997), and inorganic charge-transfer spectra (Zeng et al., 1994). The important issue here is the scaling of the quantum mechanical charges for the purpose of the molecular dynamics. Updating of solute charges in response to environmental perturbations was an integral part of the self-consistent reaction field methods using a continuum dielectric (Broo et al., 1997) and in our explicit water solvation studies (Muiño and Callis, 1994b, c), but scaling of the charges was not done in those cases. Scaling down the atomic charges was necessary for reasonable agreement with experiment in our nucleic acid crystal spectra studies. More recently, the necessity for scaling down INDO/S Löwdin excited-state charges to provide reasonable agreement with experimental gas phase dipole moments has some precedent in the class IV charge model of Truhlar and co-workers (Li et al., 2000) and references therein.

As seen in the Results section, the successes and failures of the model presented here hinge critically on the interaction of the *excited* Trp ring with water. We have also seen that the most effective computed interaction between a water and 3MI in the ^1L_a state is by H-bonding to the π cloud of the benzene ring atoms, wherein a single water creates a calculated red shift of 15 nm (1500 cm^{-1}). Note that the water (TIP3) dipole in CHARMM is larger than for an isolated water (MacKerell, Jr. et al., 1998). For a single water acting as H-bond acceptor from the indole HN (σ-complex) our calculated red shift is $\sim$10 nm. Unfortunately, these numbers cannot be easily verified experimentally for the ^1L_a state, because ^1L_a lies $\sim$500 cm^{-1} above ^1L_b in

vacuum (Sammeth et al., 1992; Short and Callis, 2000), and is therefore not the fluorescing state. Furthermore, the ^1L_a origin in the jet-cooled excitation spectrum is split into several components, making a quantitative measure of the shift difficult. In addition, only the σ-complex is observed in jet-cooled beams (Carney and Zwier, 1999). What is known is that σ-complexing with water does not invert the ^1L_a and ^1L_b states, although it does bring the two states to nearly the same energy while red-shifting the origin by 236 cm^{-1} (Demmer et al., 1994; Short and Callis, 2000). Using the observation that the ^1L_a origin components appear to be centered $\sim$500 cm^{-1} above the ^1L_b on average, this suggests the σ-bonded water red-shifts ^1L_a $\sim$740 cm^{-1} in vacuum. This translates to $\sim$7 nm, a number close to that given by the QM used here.

Another important experimental reference point comes from experiments mentioned above by Hershberger et al. (1981) who measured fluorescence from 3MI in heptane in the presence of millimolar quantities of butanol. Their data were consistent with 3MI-butanol complexes with 1:1 and 1:2 stoichiometry, causing 15 and 30 nm red shifts, respectively, of the fluorescence relative to that in pure hydrocarbon. These shifts are almost certainly a property of ^1L_a, because UV absorption (Strickland et al., 1970) and polarized two-photon excitation spectra (Sammeth, 1992) show that ^1L_a and ^1L_b are essentially degenerate for 3MI in hydrocarbon solvents. We would argue that the shift under these circumstances will be somewhat larger than in vacuum because, even in a non-polar solvent, ^1L_a is red-shifted and the change in dipole may be expected to be larger than in vacuum.

Another way of validating the INDO/S-CHARMM predictions used here is with ab initio computations. At the level of Hartree-Fock SCF and singles configuration interaction, ab initio calculated shifts are only about half those predicted by INDO/S-CIS for a given water conformation. This is also true of the effect of electric field (meaning potential difference). However, we find the electric field sensitivity of the calculated ^1L_a transition energy when using the more accurate CASPT2 (Serrano-Andres and Roos, 1996) method is similar to that shown by INDO/S. We have not yet been successful in using CASPT2 for computing a transition energy for 3MI-water complexes.

In summary, the hybrid INDO/S-CIS + MD method we are using (which includes the modification of partial charge scaling on the chromophore) is in reasonably consistent agreement with relevant experimental and theoretical information.

Effect of ignoring protein and solvent electronic polarization

Although the 3MI solute in our model shows considerable polarizability in the excited state, electronic polarization—as is normal for simulations of protein—is not included for solvent and non-Trp residues. However, the effects of polarizability are to some extent built into CHARMM and other force fields by adjusting the partial charges upward to mimic the larger dipole resulting from hydrogen bonding, for example. In addition, recent studies on model systems that include electronic polarization in molecular solvent models find little effect on energetics and solvation structure (Bader and Berne, 1996; Thompson and Schenter, 1995), while *solute* electronic polarizability exhibits striking consequences for both equilibrium and non-equilibrium solvation dynamics (Bursulaya et al., 1995). We conclude that at this point in the development of our model, the neglect of protein and solvent electronic polarizability is probably not crucially limiting the predictive power of the model.

Effect of short trajectory

There is some justifiable concern over the use of a *single* trajectory of relatively short tenure to represent, presumably, an ensemble average. The experimental analog of the computed fluorescence involves a steady-state measurement that averages over dynamics on a nanosecond or even microsecond time scale—perhaps four orders of magnitude longer than the trajectories used here—and encompassing the dynamics of $\sim 10^{20}$ individual tryptophans in their protein environments. Given the slow (few picosecond) nature of the fluctuations seen for most of the trajectories (Fig. 1), there is clearly the need for much longer trajectories to reach convergence to a $\pm$1 nm precision level. However, at this stage of the investigation, accuracy and general applicability, not precision, is of greater interest, and thus we have opted to consider a large number of proteins at a lower level of precision for this paper. For those cases deviating by $>$10 nm, further averaging is unlikely to improve the predicted value, in our opinion.

Effect of finite solvation

A reasonable concern is whether the water droplet size adequately captures the effect of bulk solvent. The choice of droplet size in this study was dictated by the compromise of two factors: 1) the requirement of complete solvation of all protein residues, and 2) size and time limitations imposed by storage and CPU. Previous results (Callis and Burgess, 1997) demonstrated that solvation of the Trp chromophore by a "patch" of only 200–300 waters yielded much the same fit as shown in Fig. 2 *A*. As a check on the size effects for the simulations in this work, we varied the droplet size for about half the proteins in Table 1 in a series of 10 ps simulations. Varying the droplet radius from 25 to 30 Å (20–30 Å for the smaller proteins) typically changed the predicted wavelength by 2–5 nm. Usually the effect was to increase the wavelength, but for phospholipaseA2 there was

an 11 nm blue shift from increasing the drop size. Our qualitative conclusion is that the finite solvation droplet contributes an error to the spectral shift of ± 5 nm and is probably no more a factor than several other limitations in the method, such as trajectory length, choice of force field parameters, and quantum mechanical method.

Why so few blue shifts from protein?

The surprising propensity for red-shifting contributions by protein means that there is a strong correlation of the local electric field and the ground state dipole direction (because the ground and ^1L_a dipoles are nearly parallel and of the same sign). Given the small ($\sim$2–3 Debye) ground state dipole there seems to be no obvious reason that the proteins would exhibit such an apparent bias. If the protein contribution to the net spectral shift were essentially random in character, blue shifts would be observed with roughly equal frequency. The probability of only three blue shifts in 19 trials is $[n\ k](\frac{1}{2})^{19} = [19\ 3](\frac{1}{2})^{19} = 1/541$, where $[n\ k]$ denotes the binomial coefficient of the coin-toss (Bernoulli trial) experiment considered here. This reinforces what the shift contribution result in Fig. 3 strongly suggests, i.e., that the orientation of the Trps in our sample is highly correlated with the electric field direction.

Two possible speculations for the origin of this correlation may be offered at this point: The first is that even the relatively modest ground state dipole of the Trp ring could contribute unacceptable instability for proper folding. Support for this is that a 10^7 v/cm field (typical of fields we compute) combined with a 2 Debye dipole gives an energy of $\sim$1 kcal/mol. The energy difference with the Trp orientation such that the field destabilizes the dipole compared to one that maximally stabilizes it is therefore on the order of 2 kcal/mol, a value on the order of 10% of a typical Gibbs free energy change for folding. In terms of a barrier, this translates into a 25-fold decrease in folding rate. From an equilibrium point of view, the equilibrium constant would be 25-fold smaller, and would typically shift the denaturation temperature by tens of degrees centigrade. Supporting this line of argument are some preliminary results we have completed on this same set of Trps and proteins wherein the trajectories were begun after changing χ_2 of the Trp by 180° from its PDB structure value. The results for this yielded protein contributions to the wavelengths that were much less biased toward red-shifting.

A second possibility requires dismissing the above thermodynamic arguments and concluding that our sample of proteins taken from a list of single-Trp proteins with known fluorescence properties (Eftink, 1991) is strongly biased. One obvious bias is that these Trps all fluoresce well enough to be easily studied, suggesting that Trps oriented in a destabilizing way relative to the field have extremely low fluorescence quantum yields. However, experimental fluorescence properties (Eftink, 1991) for the proteins examined here show no correlation between the emission maximum and quantum yield.

Consequence of ionization choices

The results given in this paper are for every histidine, tyrosine, and cysteine in the neutral form, all glutamates and aspartates in the anion form, and all lysines and arginines in the cation form. The pK_a for the histidine side chain in aqueous solution is 6, and that for tyrosine is 10.1. Thus, our results are nominally equivalent to a pH of $\sim$7.5–8.5. However, the large deviations of electrical potential that affect the Trp fluorescence wavelength also perturb the pK_a values of these residues (Sham et al., 1997). pK_a values for histidines range from 5 to 8 (Sham et al., 1997) in proteins, so that if we are striving to predict the fluorescence spectrum at pH 7, there will occasionally be histidines that are substantially protonated. One case for which this is likely to have an impact is for Trp-48 of apo-azurin, which has the same λ_{max} as the holo (Cu^{2+}) protein. Of the five histidines, three would give a sizable blue shift if protonated (based on their position relative to the Trp ring), and those three are the ones complexed with the Cu^{2+} in the holoenzyme. The other two would give only a small red shift, if any. Most likely, at least two of the histidines that bind the Cu^{2+} would be protonated. Similarly, if His-48 of phospholipase A2 were protonated, one can estimate that the calculated λ_{max} would be $\sim$5 nm closer to the experimental value. In subtilisin C all histidines would be red-shifting if protonated. Asp-26 of oxidized thioredoxin is located in van der Waals contact of the pyrrole ring of Trp-28 and is known to have a pK_a of 7.5 (Langsetmo et al., 1991), shifted $\sim$3 pK_a units from the normal value because of its relatively buried environment. Thus, our simulation is consistent with a pH of $\sim$8.5 for this protein. As an anion, Asp-26 contributes a 60 nm red shift, which is offset by nearby blue-shifting residues. Experimentally, there is only about a 5 nm blue shift in λ_{max} when the pH is taken to 6 (Callis et al., 2000), indicating that perhaps movement of Lys-57 or changes in solvation compensate for the large loss of charge upon protonation.

SUMMARY AND CONCLUSIONS

The inclusion of complete solvation, 30-ps trajectories, crystallographic waters, metal ions, and charge scaling have improved our ability to predict the fluorescence peak wavelength of tryptophan in proteins. This study has solidified the notion that the wavelength is determined primarily by the electrical potential difference across the long axis of the indole ring. This means that the relative direction of a charge from the Trp ring is crucial: positive charges create a red shift when on the benzene ring end and a blue shift when on the pyrrole ring end, with the size of the shift being

inversely proportional to the distance from the center of the Trp ring. The reverse is true for negative charges.

The combination of the CHARMM22 force field, explicit water and INDO/S Löwdin charges on Trp (scaled by 0.80), and ab initio geometry difference (CIS-HF/3–21G) gives a good quantitative prediction for the fluorescence wavelength maximum, with the only fitting parameter being the charge scaling factor for the Trp ring. No protein dielectric constant was imposed.

Both water and protein contribute in various ratios to the shift, but the ratio is in most cases difficult to anticipate. When charged groups lie close to Trp, they usually dominate the mechanism of the shift, and waters may even create a *blue shift* in such environments.

Water exposure, per se, is not sufficient for a red shift. If the exposure is only along one edge of the Trp, only modest red shifts from water are possible. However, if one or both faces of the benzene ring are water-exposed, the wavelength of the fluorescence peak is usually near 350 nm. In such cases a few waters make particularly large red shifts (~20 nm) due to exciplex-like H-bonds with negatively charged C atoms of the benzene ring in the ^1L_a excited state.

Water may cause significant (10–20 nm) red shifts for Trps that are essentially *buried*. This appears to be due to the collective action of regions of water up to 25 nm distant that are probably oriented by the charges and/or shape of the protein.

The extreme red-shifting bias of the protein contributions is surprising. It suggests that protein electric fields relative to the modest ground state dipole of the Trp residue may be important.

This work provides evidence that the CHARMM22 and CVFF force fields give a reasonably accurate account of local electric fields in proteins, and complements work aimed at predicting pK_a values and redox potentials, which are sensitive to long-range potential differences.

The method described here can be easily extended to gain insight about environmental effects on the absorption and fluorescence of other chromophores and environments, e.g., Trp in membranes, green fluorescent protein, and other probes. In particular, it should be useful for interpreting changes in Trp fluorescence wavelengths during protein folding/unfolding dynamics (Ervin et al., 2000).

The use of the method reported here has deliberately been reduced in depth to gather an overview of several proteins. We plan several more penetrating and focused studies on individual proteins through further analysis of data in hand and from additional simulations. Work is in progress to predict the effect of different protonation states, Trp rotamer variations, and counterions. We also plan to apply the method to other proteins, including the behavior at lipid-water surfaces.

Note added in proof. All predicted wavelengths are simply the reciprocal of the energy (wavenumber) without correction for radiative rate (λ^{-3}) and the effect of wavelength dispersion (λ^{-2}). These corrections would reduce the predicted wavelengths by 6–8 nm. All wavelength *shifts* were computed from energy shifts assuming a wavelength of 310 nm.

This work was made possible by National Science Foundation Grant MCB9817372 and benefited from an allotment of CPU time on the SGI Origin2000 at the Center for Computational Biology, Montana State University.

We thank Dr. Dimitri Toptygin for helpful comments.

REFERENCES

Andrews, L. J., and L. S. Forster. 1972. Protein difference spectra. Effect of solvent and charge on tryptophan. *Biochemistry.* 11:1875–1879.

Axelsen, P. H., and F. G. Prendergast. 1989. Molecular dynamics of tryptophan in ribonuclease-T1. II. Correlations with fluorescence. *Biophys. J.* 56:43–66.

Bader, J. S., and B. J. Berne. 1996. Solvation energies and electronic spectra in polar, polarizable media: simulation tests of dielectric continuum theory. *J. Chem. Phys.* 104:1293–1308.

Beechem, J. M., and L. Brand. 1985. Time-resolved fluorescence of proteins. *Annu. Rev. Biochem.* 54:43–71.

Berman, H. M., J. Westbrook, Z. Feng, G. Gilliland, T. N. Bhat, I. N. Shindyalov, and P. N. Bourne. 2000. The Protein Data Bank. *Nucleic Acids Res.* 28:235–242.

Broo, A., G. Pearl, and M. C. Zerner. 1997. Development of a hybrid quantum chemical and molecular mechanics method with application to solvent effects on the electronic spectra of uracil and uracil derivatives. *J. Phys. Chem. A.* 101:2478–2488.

Burstein, E. A., N. S. Vedenkina, and M. N. Ivkova. 1973. Fluorescence and the location of tryptophan residues in protein molecules. *Photochem. Photobiol.* 18:263–279.

Burstein, E. A., E. A. Permyakov, V. A. Yashin, S. A. Burkhanov, and A. Finazzi-Agro. 1977. The fine structure of luminescence spectra of azurin. *Biochim. Biophys. Acta.* 491:155–159.

Bursulaya, D. A., D. A. Zichi, and H. J. Kim. 1995. Role of solute electronic polarizability in solvation dynamics. *J. Phys. Chem.* 99: 10069–10074.

Callis, P. R. 1984. Transition density topology of the La and Lb states of indoles and purines. *Int. J. Quantum Chem.* S18:579–588.

Callis, P. R. 1991. Molecular orbital theory of the ^1L_a and ^1L_b states of indole. *J. Chem. Phys.* 95:4230–4240.

Callis, P. R. 1997. ^1L_a and ^1L_b transitions of tryptophan: applications of theory and experimental observations to fluorescence of proteins. *Methods Enzymol.* 278:113–150.

Callis, P. R., and B. K. Burgess. 1997. Tryptophan fluorescence shifts in proteins from hybrid simulations: an electrostatic approach. *J. Phys. Chem.* 101:9429–9432.

Callis, P. R., W. R. Kirk, and F. G. Prendergast. 2000. pH-Induced fluorescence shifts in *E. coli* thioredoxin mutants. Comparison of experiment and theory. *Biophys. J.* 78:127*a*. (Abstr.).

Callis, P. R., and A. A. Rehms. 1993. Two-photon fluorescence excitation spectra of aromatic amino acids. *Chem. Phys. Lett.* 208:276–282.

Callis, P. R., J. T. Vivian, and L. S. Slater. 1995. Ab initio calculations of vibronic spectra for indole. *Chem. Phys. Lett.* 244:53–58.

Carney, J. R., and T. S. Zwier. 1999. Infrared and ultraviolet spectroscopy of water-containing clusters of indole, 1-methylindole, and 3-methylindole. *J. Phys. Chem.* 103:9943–9957.

Chabalowski, C. F., D. R. Garmer, J. O. Jensen, and M. Krauss. 1993. Reaction field calculation of the spectral shifts of indole. *J. Phys. Chem.* 97:4608–4613.

Chen, Y., and M. D. Barkley. 1998. Toward understanding tryptophan fluorescence in proteins. *Biochemistry.* 37:9976–9982.

Demchenko, A. P. 1986. Ultraviolet Spectroscopy of Proteins. Springer-Verlag, New York.

Demmer, D. R., G. W. Leach, and S. C. Wallace. 1994. ^1L_a-^1L_b coupling in the excited state of 3-methylindole and its polar clusters. *J. Phys. Chem.* 98:12834–12843.

Eftink, M. R. 1991. Fluorescence techniques for studying protein structure. *Methods Biochem. Anal.* 35:127–205.

Egan, D. A., T. M. Logan, H. Liang, E. Matayoshi, S. W. Fesik, and T. F. Holzman. 1993. Equilibrium denaturation of recombinant human FK binding protein in urea. *Biochemistry.* 32:1920–1927.

Ervin, J., J. Sabelko, and M. Gruebele. 2000. Submicrosecond real-time fluorescence sampling: application to protein folding. *J. Photochem. Photobiol. B.* 54:1–15.

Fender, B. J., and P. R. Callis. 1996. ^1L_a origin locations of methylindoles in argon matrices. *Chem. Phys. Lett.* 262:343–348.

Fender, B. J., D. M. Sammeth, and P. R. Callis. 1995. Site selective photoselection study of indole in argon matrix: location of the ^1L_a origin. *Chem. Phys. Lett.* 239:31–37.

Fender, B. J., K. W. Short, D. K. Hahn, and P. R. Callis. 1999. Vibrational assignments for indole with the aid of ultrasharp phosphorescence spectra. *Int. J. Quantum Chem.* 72:347–356.

Florian, J., and A. Warshel. 1997. Langevin dipoles model for ab initio calculations of chemical processes in solution: parameterization and application to hydration free energies of neutral and ionic solutes and conformational analysis in aqueous solutions. *J. Phys. Chem. B.* 101: 5583–5595.

Gehlen, J. N., M. Marchi, and D. Chandler. 1994. Dynamics affecting the primary charge transfer in photosynthesis. *Science.* 263:499–502.

Hahn, D. K., and P. R. Callis. 1997. The lowest triplet state of indole: an ab initio study. *J. Phys. Chem.* 101:2686–2691.

Harris, D. L., and B. S. Hudson. 1991. Fluorescence and molecular dynamics study of the internal motion of the buried tryptophan in bacteriophage T4 lysozyme: effects of temperature and alteration of nonbonded networks. *Chem. Phys.* 158:353–382.

Hayes, D. M., and P. A. Kollman. 1976. Electrostatic potentials of proteins. 2. Role of electrostatics in a possible catalytic mechanism for carboxypeptidase A. *J. Am. Chem. Soc.* 98:7811–7816.

Hershberger, M. V., R. Lumry, and R. Verrall. 1981. The 3-methylindole/n-butanol exciplexes: evidence for two exciplex sites in indole compounds. *Photochem. Photobiol.* 33:609–617.

Higo, J., H. Kono, N. Nakajima, H. Shirai, H. Nakamura, and A. Sarai. 1999. Molecular dynamics study on mobility and dipole ordering of solvent around proteins: effects of periodic-box size and protein charge. *Chem. Phys. Lett.* 306:395–401.

Honig, B., U. Dinur, K. Nakanishi, V. Balogh-Nair, M. A. Gawinowicz, M. Arnaboldi, and M. G. Motto. 1979. An external point-charge model for wavelength regulation in visual pigments. *J. Am. Chem. Soc.* 101: 7084–7086.

Honig, B., and A. Nicholls. 1995. Classical electrostatics in biology and chemistry. *Science.* 268:1144–1149.

Ilich, P., and F. G. Prendergast. 1991. Electronic states of the indole-acrylamide molecular pair. *Photochem. Photobiol.* 53:445–453.

Jimenez, R., G. R. Fleming, P. V. Kumar, and M. Maroncelli. 1994. Femtosecond solvation dynamics of water. *Nature.* 369:471–473.

Kohler, B. E., and J. C. Woehl. 1995. Measuring internal fields with atomic resolution. *J. Chem. Phys.* 102:7773–7781.

Konev, S. V. 1967. Fluorescence and Phosphorescence of Proteins and Nucleic Acids. Plenum, New York.

Lakowicz, J. 1999. Principles of Fluorescence Spectroscopy. Plenum, New York.

Langsetmo, K., J. A. Fuchs, and C. Woodward. 1991. The conserved, buried aspartic acid in oxidized *E. coli* thioredoxin has a pK_a of 7.5. Its titration produces a related shift in global stability. *Biochemistry.* 30: 7603–7609.

Li, J., T. Zhu, C. J. Cramer, and D. G. Truhlar. 2000. New class IV charge model for extracting accurate partial charges from wave functions. *J. Phys. Chem. A.* 102:1820–1831.

Lifson, S., A. T. Hagler, and P. Dauber. 1979. Consistent force field studies of intermolecular forces in hydrogen-bonded crystals. 1. Carboxylic acids, amides, and the C═O. . . H– hydrogen bonds. *J. Am. Chem. Soc.* 101:5111–5121.

Lockhart, D. J., and P. S. Kim. 1992. Internal Stark effect measurement of the electric field at the amino terminus of an alpha helix. *Science.* 257:947–951.

Lockhart, D. J., and P. S. Kim. 1993. Electrostatic screening of charge and dipole interactions with the helix backbone. *Science.* 260:198–202.

Longworth, J. W. 1971. Luminescence of polypetides and proteins. *In* Excited States of Proteins and Nucleic Acids. R. F. Steiner and I. Weinryb, editors. Plenum, New York. 319–483.

Lyne, P. D., M. Hodoscek, and M. Karplus. 1999. A hybrid QM-MM potential employing Hartree-Fock or density functional methods in the quantum region. *J. Phys. Chem. A.* 103:3462–3471.

MacKerell, A. D., Jr., D. Bashford, M. Bellott, R. L. Dunbrack, J. D. Evanseck, M. J. Field, S. Fischer, J. Gao, S. Ha, D. Joseph-McCarthy, L. Kuchnir, K. Kuczera, F. T. K. Lau, C. Mattos, S. Michnick, T. Ngo, D. T. Nguyen, B. Prodhom, W. E. Reiher III, B. Roux, M. Schlenkrich, J. C. Smith, R. Stote, J. Straub, M. Watanabe, J. Wiorkiewicz-Kuczera, D. Yin, and M. Karplus. 1998. All-atom empirical potential for molecular modeling and dynamics studies of proteins. *J. Phys. Chem. B.* 102:3586–3616.

Marchi, M., J. N. Gehlen, D. Chandler, and M. Newton. 1993. Diabatic surfaces and the pathway for primary electron transfer in a photosynthetic reaction center. *J. Am. Chem. Soc.* 115:4178–4190.

Maroncelli, M. 1993. The dynamics of solvation in polar liquids. *J. Mol. Liquids.* 57:1–37.

Mataga, N., Y. Torihashi, and K. Ezumi. 1964. Electronic structures of carbazole and indole and the solvent effects on the electronic spectra. *Theor. Chim. Acta (Berlin).* 2:158–167.

Muiño, P. L., and P. R. Callis. 1994a. ^1L_a transitions of jet-cooled indoles and complexes from two-photon fluorescence excitation. *Proc. SPIE-Int. Soc. Opt. Eng.* 2137:278–287.

Muiño, P. L., and P. R. Callis. 1994b. Hybrid simulations of solvation effects on electronic spectra: indoles in water. *J. Chem. Phys.* 100: 4093–4109.

Muiño, P. L., and P. R. Callis. 1994c. Simulations of solvent effects on fluorescence spectra and dynamics of indoles. *Proc. SPIE-Int. Soc. Opt. Eng.* 2137:362–371.

Muiño, P. L., D. Harris, J. Berryhill, B. Hudson, and P. R. Callis. 1992. Simulation of solvent dynamics effects on the fluorescence of 3-methylindole in water. *Proc. SPIE-Int. Soc. Opt. Eng.* 1640:240–250.

Onsager, L. 1936. Electric moments of molecules in liquids. *J. Am. Chem. Soc.* 58:1486–1493.

Pierce, D. W., and S. G. Boxer. 1995. Stark effect spectroscopy of tryptophan. *Biophys. J.* 68:1583–1591.

Rehms, A. A., and P. R. Callis. 1987. Resolution of La and Lb bands in methyl indoles by two-photon spectroscopy. *Chem. Phys. Lett.* 140: 83–89.

Reshetnyak, Ya. K., and E. A. Burstein. 1997. Assignment of the components of the fluorescence spectrum of protein to tryptophan residues based on the properties of their microenvirons in a three dimensional structure. *Biophysics.* 42:267–274.

Ridley, J., and M. Zerner. 1973. Intermediate neglect of differential overlap (INDO) technique for spectroscopy: pyrrole and the azines. *Theor. Chim. Acta (Berlin).* 32:111–134.

Ryckaert, J. P., G. Cicotti, and H. J. C. Berendsen. 1977. Numerical integration of Cartesian equations of motion of a system with constraints: molecular dynamics of n-alkanes. *J. Comp. Phys.* 23: 327–341.

Sammeth, D. M. 1992. Polarized two-photon fluorescence excitation studies of jet- cooled indoles. Ph.D. Thesis, Montana State University.

Sammeth, D. M., S. S. Siewert, L. H. Spangler, and P. R. Callis. 1992. ^1L_a transitions of jet-cooled 3-methylindole. *Chem. Phys. Lett.* 193: 532–538.

Sammeth, D. M., S. Yan, L. H. Spangler, and P. R. Callis. 1990. Two-photon fluorescence excitation spectra of indole in vapor and jet: ^1L_a states. *J. Phys. Chem.* 94:7340–7342.

Serrano-Andres, L., and B. O. Roos. 1996. Theoretical study of the absorption and emission spectra of indole in gas phase and solvent. *J. Am. Chem. Soc.* 118:185–195.

Sham, Y. Y., Z. T. Chu, and A. Warshel. 1997. Consistent calculations of pKa's of ionizable residues in proteins: semi-microscopic and microscopic approaches. *J. Phys. Chem. B.* 101:4458–4472.

Sham, Y. Y., I. Muegge, and A. Warshel. 1998. The effect of protein relaxation on charge-charge interactions and dielectric constants of proteins. *Biophys. J.* 74:1744–1753.

Short, K. W., and P. R. Callis. 2000. Studies of jet-cooled 3-methylindole-polar solvent complexes: identification of ^1L_a fluorescence. *J. Chem. Phys.* 113:5235–5244.

Simonson, T., C. F. Wong, and A. T. Bruenger. 1997. Classical and quantum simulations of tryptophan in solution. *J. Phys. Chem. A.* 101: 1935–1945.

Sitkoff, D., D. J. Lockhart, K. A. Sharp, and B. Honig. 1994. Calculation of electrostatic effects at the amino terminus of an alpha helix. *Biophys. J.* 67:2251–2260.

Skalski, B., D. M. Rayner, and A. G. Szabo. 1980. Ground-state complexes between polar solvents and 1-methylindole: the origin of the Stokes shift in their fluorescence spectra. *Chem. Phys. Lett.* 70:587–590.

Slater, L. S., and P. R. Callis. 1995. Molecular orbital theory of the ^1L_a and ^1L_b states of indole. 2. An ab initio study. *J. Phys. Chem.* 99:8572–8581.

Sreerama, N., R. W. Woody, and P. R. Callis. 1994. Theoretical study of the crystal field effects on the transition dipole moments in methylated adenines. *J. Phys. Chem.* 98:10397–10407.

Strickland, E. H., J. Horwitz, and C. Billups. 1970. Near-ultraviolet absorption bands of tryptophan. Studies using indole and 3-methylindole as models. *Biochemistry.* 9:4914–4920.

Szabo, A. G., T. M. Stepanik, D. M. Wayner, and N. M. Young. 1983. Conformational heterogeneity of the copper binding site in azurin. *Biophys. J.* 41:233–244.

Takigawa, T., T. Ashida, Y. Sasada, and M. Kakudo. 1966. The crystal structures of L-tryptophan hydrochloride and hydrobromide. *Bull. Chem. Soc. Jpn.* 39:2369–2378.

Tannor, D. J., B. Marten, R. Murphy, R. A. Friesner, D. Sitkoff, A. Nicholls, M. Ringnala, W. A. Goddard III, and B. Honig. 1994. Accurate first principles calculation of molecular charge distributions and solvation energies from ab initio quantum mechanics and continuum dielectric theory. *J. Am. Chem. Soc.* 116:11875–11882.

Theiste, D., P. R. Callis, and R. W. Woody. 1991. Effects of the crystal field on transition moments in 9-ethylguanine. *J. Am. Chem. Soc.* 113: 3260–3267.

Thompson, M. A., and G. K. Schenter. 1995. Excited states of the bacteriochlorophyll *b* dimer of *Rhodopseudomonas viridis:* a QM/MM study of the photosynthetic reaction center that includes MM polarization. *J. Phys. Chem.* 99:6374–6386.

Thompson, M. A., and M. C. Zerner. 1991. A theoretical examination of the electronic structure and spectroscopy of the photosynthetic reaction center from *Rhodopseudomonas viridis*. *J. Am. Chem. Soc*. 113: 8210–8215.

Varadarajan, R., D. G. Lambright, and S. G. Boxer. 1989. Electrostatic interactions in wild-type mutant recombinant human myoglobins. *Biochemistry.* 28:3771–3781.

Verlet, L. 1967. Computer "experiments" on classical fluids. I. Thermodynamic properties of Lennard-Jones molecules. *Phys. Rev.* 159: 98–108.

Walker, M. S., T. W. Bednar, and R. Lumry. 1967. Excited-state solute-solvent complex studies. II. Indole and indole derivatives. *J. Chem. Phys.* 47:1020–1028.

Warshel, A. 1991. Computer modeling of chemical reactions in enzymes and solutions. Wiley-Interscience, New York, NY.

Warshel, A., and J. Aqvist. 1991. Electrostatic energy and macromolecular function. *Annu. Rev. Biophys. Biophys. Chem.* 20:267–298.

Weber, G. 1960. Fluorescence-polarization spectrum and electronic energy transfer in tyrosine, tryptophan and related compounds. *Biochem J.* 75:335–345.

Zeng, J., J. S. Craw, N. S. Hush, and J. R. Reimers. 1994. Solvent effects on molecular and ionic spectra. 4. Photochemistry of $Fe^{2+}(H_2O)_6$ in water revisited: possible mechanisms for the primary absorption process leading to electron ejection. *J. Phys. Chem.* 98:11075–11088.